Effects of TiO2 Addition on Microstructure and Ionic Conductivity of Gadolinia-Doped Ceria

Journal:	*39th Int'l Conf & Expo on Advanced Ceramics & Composites (ICACC 2015)*
Manuscript ID:	2059940.R1
Symposium:	SYMPOSIUM 3: 11th International Symposium on Solid Oxide Fuel Cells (SOFC): Materials, Science and Technology
Date Submitted by the Author:	n/a
Complete List of Authors:	Muccillo, Eliana
Keywords:	

EFFECTS OF TiO_2 ADDITION ON MICROSTRUCTURE AND IONIC CONDUCTIVITY OF GADOLINIA-DOPED CERIA SOLID ELECTROLYTE

M. C. F. Dias and E. N. S. Muccillo
Energy and Nuclear Research Institute
PO Box 11049, Pinheiros, S. Paulo, 05422-970, SP, Brazil

ABSTRACT

Ceria containing trivalent rare-earth is a solid electrolyte with higher ionic conductivity than the yttria fully-stabilized zirconia standard ionic conductor. This feature turns these ceria-based ionic conductors promising materials for application in solid oxide fuel cells operating at intermediate temperatures (500-700ºC). One of the most utilized approaches to optimize the electrical conductivity and other properties of these materials is the introduction of a second additive. In this work, ceria-20 mol% gadolinia with additions of TiO_2 was prepared by solid state reaction. The main purpose was to investigate the effects of the additive on densification, microstructure and electrical conductivity of the solid electrolyte. Sintered pellets were characterized by evaluating apparent density, X-ray diffraction, Raman spectroscopy, scanning electron microscopy, and electrical conductivity by impedance spectroscopy. The additive was found to influence all studied properties. Increase of densification was obtained with TiO_2 addition. This additive promotes increase of the blocking of charge carriers at the grain boundaries due to solute exsolution and formation of the pyrochlore $Gd_2Ti_2O_7$ phase at grain boundaries for contents in excess of the solubility limit.

INTRODUCTION

Polycrystalline ceramics based on cerium dioxide have attracted much attention over the last decades from both theoretical and experimental point of views, due to their wide range of applications. Some of the well know applications of cerium-based ceramics are as catalysts for chemical reactions [1], mechanical polishing media in microelectronics [2], as gas sensor [3], as solid electrolyte and electrode in solid oxide fuel cells [4], luminescent material [5] and as ultraviolet filter and blocker [6,7].

Additives in cerium dioxide have been used for changing a specific property. The addition of trivalent rare earth, for example, results in a substantial increase of the ionic conductivity. The highest increase of the ionic conductivity in cerium dioxide based solid solutions has been obtained with samarium and gadolinium. The ionic conductivity of Gd-doped ceria at 800ºC is similar to that of yttria-stabilized zirconia at 1000ºC [8]. Thus, these solid solutions have been considered for possible application in solid oxide fuel cells operating at intermediate temperatures (600-800ºC) [8].

Other additives to cerium oxide ceramics have been considered to aid the sintering process allowing for increasing the sinterability of this material along with a better microstructural design and control. Few reports may be found concerning the addition of TiO_2 to doped ceria ceramics, probably because the partial substitution of Ce^{4+} for Ti^{4+} do not change the concentration of oxygen vacancies. Consequently, no influence of this additive on the ionic conductivity is expected. Jurado [9] showed that titanium oxide addition do gadolinia-doped ceria introduces a low resistivity intergranular phase, thereby the blocking of charge carriers at the grain boundaries is reduced. Cutler [10] and Pikalova [11] observed an increased densification of doped ceria with this additive. The latter also observed that a pirochlore phase with composition $Gd_2Ti_2O_7$ was formed depending on the content of TiO_2.

In this work, the effects of TiO_2 on the densification, microstructure and ionic conductivity of gadolinia-doped ceria was investigated, for additive contents below and above its solubility limit.

EXPERIMENTAL

$Ce_{0.8}Gd_{0.2}O_{2-\delta}$, CGO (>99.5%, Fuel Cell Materials) and TiO_2 (99.95%, Alfa Aesar) were used as starting materials. Solid solutions containing 1, 2.5 and 5 mol% TiO_2 were prepared by solid state reaction. The starting materials were first dried in an oven. Afterwards they were mixed in alcoholic medium in the stoichiometric proportions. After drying, the mixtures were pressed into discs of 10 mm diameter and 2-3 mm thickness. Sintering was performed in a box type furnace (Lindberg BlueM) heating at a rate of 3 ºC.min^{-1} up to 1100ºC and at 5 ºC.min^{-1} from 1100 to 1500ºC with 3 h holding time. For comparison purposes, specimens without the additive were also prepared under the same experimental conditions.

Characterization of the sintered specimens was carried out by density measurements using the immersion method. The porosity of the sintered materials was estimated according to ASTM C20-00. The phases were characterized by Raman spectroscopy (Renishaw, InVia Raman Microscope) with a He-Ne laser with 633 nm wavelength in the 200-800 cm^{-1} spectral range. The microstructure of polished and thermally etched surfaces was evaluated by scanning electron microscopy (Philips, XL30) with secondary electrons. The electrical conductivity was determined by impedance spectroscopy measurements (HP 4192A) in the 5 Hz-13 MHz frequency range. Silver was used as electrode material.

RESULTS AND DISCUSSION

All sintered specimens attained high density values as shown in Table 1. Addition of TiO_2 allowed for increasing further the density, turning negligible the apparent porosity.

Table 1. Values of relative density and apparent porosity of sintered specimens.

Material	Relative density (%)	Porosity (%)
CGO	97.5	0.1
CGO + 1% TiO_2	99.8	~ 0
CGO + 2.5% TiO_2	98.7	~ 0
CGO + 5% TiO_2	~ 100	~ 0

The linear shrinkage up to 1500ºC (not shown here) is similar for both specimens (with and without titanium oxide) and amounts 23%. In addition, the additive does not change the initial temperature of shrinkage.

Figure 1 shows Raman spectra of the investigated specimens.

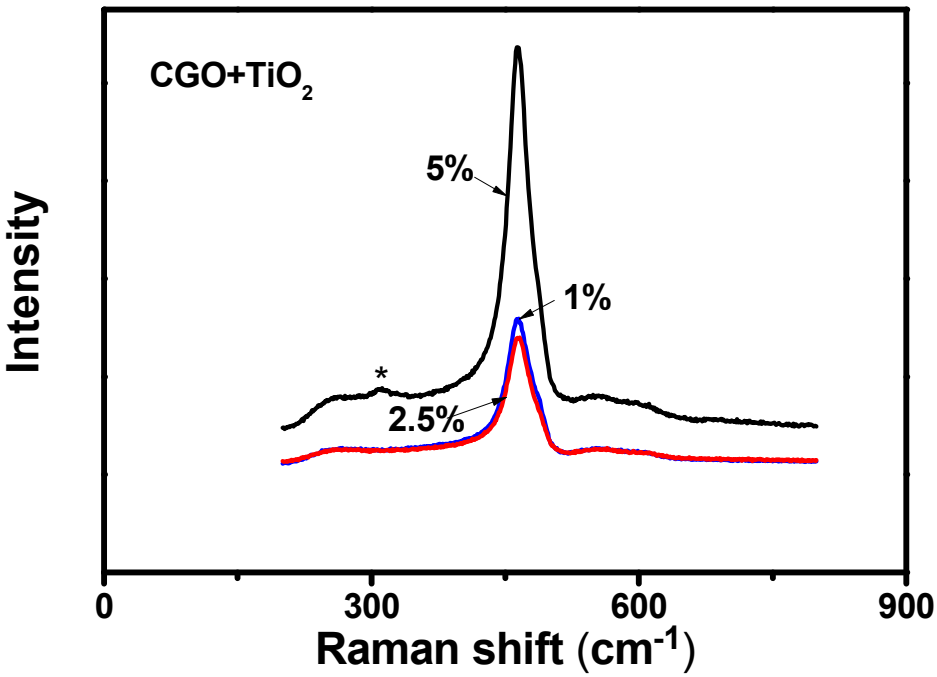

Figure 1. Raman spectra of sintered specimens containing TiO_2.

The Raman spectra consist of a predominant band centered at 465 cm^{-1} attributed to the triple degenerated F_{2g} mode of the fluorite lattice. Low intensity Raman bands at 550 and 650 cm^{-1} are usually assigned to the extrinsic oxygen vacancies created by partial substitutions [12]. In the Raman spectrum of the specimen containing 5 mol% TiO_2, other low intensity band at ~ 312 cm^{-1} is observed (indicated by *). This band is ascribed to $Gd_2Ti_2O_7$ phase, which displays about six allowed Raman modes [13]. This result evidences then the formation of the pirochlore phase in specimens with 5 mol% TiO_2. Moreover, the formation of this crystalline secondary phase reveals that when the concentration of the additive exceeds the solubility limit in the ceria matrix, it induces the exsolution of the dopant (gadolinium) from the solid solution. It is worth noting that no other phase than the cubic fluorite characteristic of ceria was detected by conventional X-ray diffraction measurements, possibly due to the experimental limitations of that technique.

Figure 2 shows a scanning electron microscopy micrograph (a) and an impedance spectroscopy diagram of the base material after sintering at 1500ºC for 3 h.

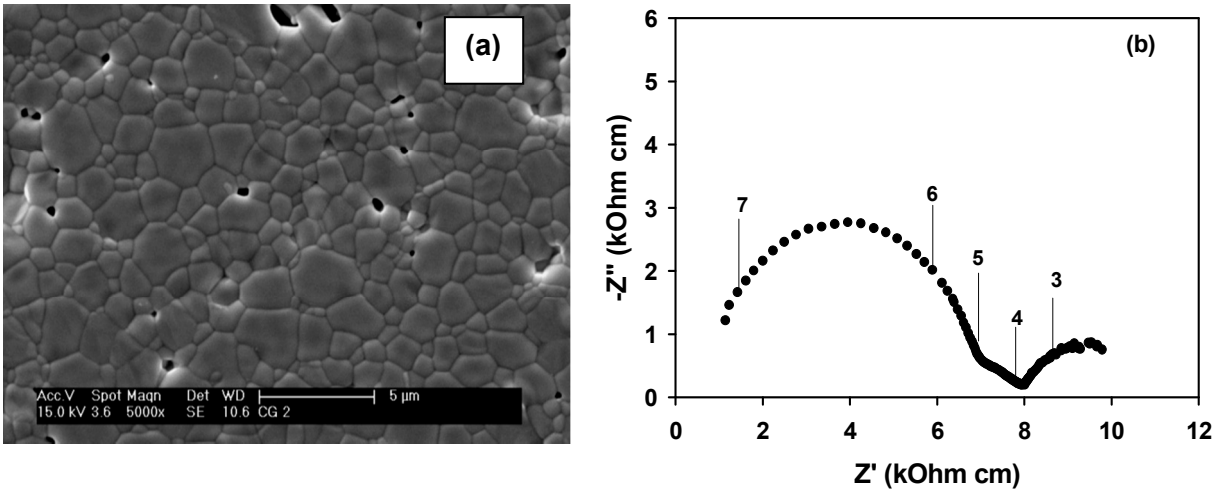

Figure 2. (a) scanning electron microscopy micrograph and (b) impedance spectroscopy diagram of gadolinia-doped ceria. In (b) numbers stand for the logarithm of the frequency (Hz). Temperature of measurement = 310ºC.

A highly dense ceramic with low fraction of pores, mostly confined at triple grain junctions, may be seen in this micrograph. The grain size distribution is relatively wide consisting of grains in the submicron and micron size ranges. The grains show a polygonal shape. The impedance spectroscopy diagram of this specimen measured at 310ºC shows a high frequency semicircle due to the capacitive and resistive effects of grains, and a low intensity one in the intermediate frequency range, attributed to the blocking of charge carriers at the grain boundaries. In the low frequency range, the reactions occurring at the interface electrode/electrolyte give rise to a third semicircle. This impedance diagram evidences the relatively negligible effect of the grain boundaries compared to previous reports [14-16].

Figure 3 shows (a-c) the scanning electron microscopy micrographs of specimens containing TiO_2 and (d) the impedance spectroscopy diagrams. All specimens with TiO_2 show very low fraction of porosity and negligible pullout. The mean grain size increases with increasing the content of the additive. The composition with 5 mol% TiO_2 exhibits small grains along the grain boundaries. These small sized grains are probably related to the pirochlore $Gd_2Ti_2O_7$ phase detected for this specimen by Raman spectroscopy (Figure 1). In the micrograph of the specimens with 2.5 mol% TiO_2 (b) these small sized grains are also observed. Then, the pirochlore phase was not detected by Raman spectroscopy in this specimen possibly due to its small content. Therefore, the solute exsolution effect due to addition of titania to gadolinia-doped ceria should occur whenever the concentration of titania exceeds its solubility limit (about 1.2 mol% [11]) in the matrix. It is interesting to note the evolution of the grain size in these micrographs. The additive promotes densification by grain growth for titania contents up to 2.5 mol%, and for higher concentrations, the formed new phase act as pinning points along the grain boundaries, inhibiting grain growth.

The impedance spectroscopy diagrams shown in Figure 3d reveal that the grain and the grain boundaries are influenced by the additive.

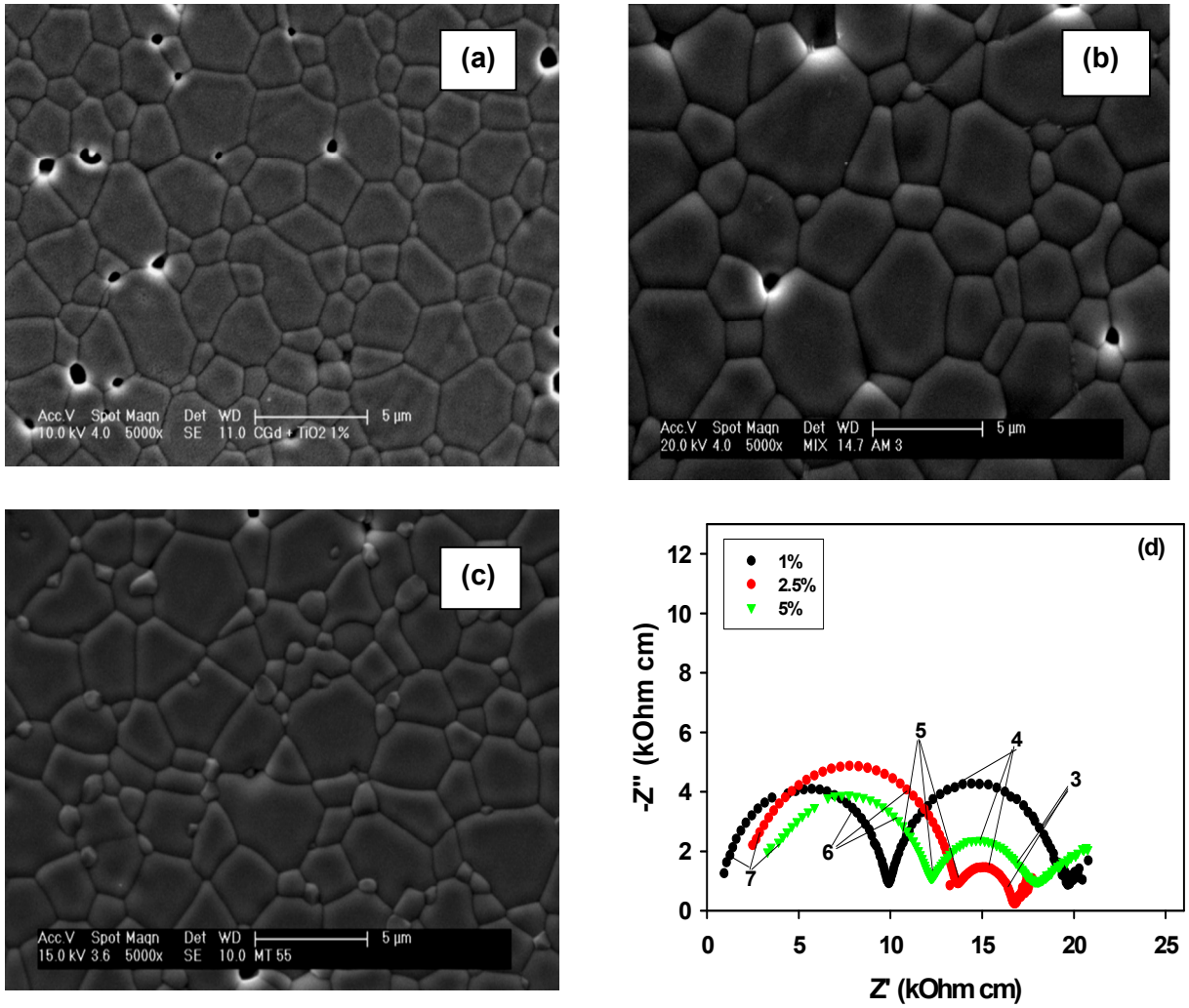

Figure 3. Scanning electron microscopy micrographs of gadolinia-doped ceria with (a) 1, (b) 2.5 and (c) 5 mol% TiO_2, and (d) impedance spectroscopy diagrams measured at 310ºC.

The Arrhenius plots of grains and grain boundaries for gadolinia-doped ceria are shown in Figure 4. A single straight line in these plots ensures that no change in the conduction mechanism occurs in the temperature range of measurements. Moreover, the straight lines are parallel to each other evidencing similar activation energy for conduction of both grains and grain boundaries. Table 2 lists activation energy values determined for grain (E_g) and grain boundaries (E_{gb}).

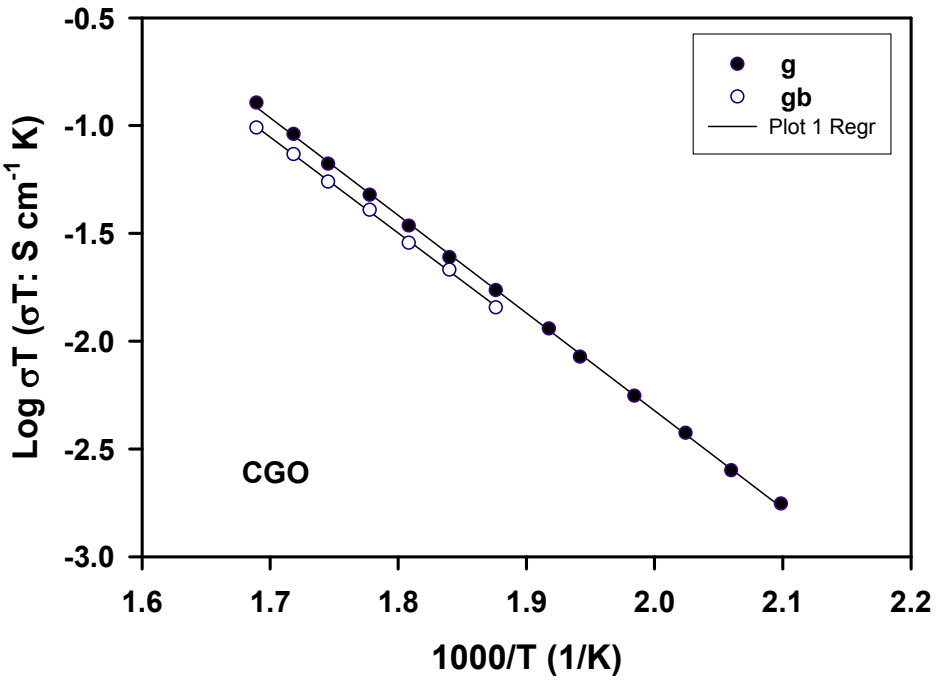

Figure 4. Arrhenius plots of the grain and grain boundary conductivity in gadolinia-doped ceria.

Table 2. Values of activation energy for grain (E_g) and grain boundary (E_{gb}) conduction.

Material	E_g (eV)	E_{cg} (eV)
CGO	0.89 ± 0.05	0.88 ± 0.05
CGO + 1% TiO_2	0.88 ± 0.05	0.95 ± 0.05
CGO + 2.5% TiO_2	0.91 ± 0.05	0.97 ± 0.05
CGO + 5% TiO_2	0.88 ± 0.05	0.91 ± 0.05

The Arrhenius plots of grain and grain boundary conductivities of TiO_2 containing gadolinia-doped ceria are shown in Figure 5. The grain conductivity (a) shows a slight dependence with the content of TiO_2, which is a further evidence of the low solubility limit of this additive in the ceria matrix. The blocking of charge carriers at the grain boundaries decreases from 1 to 2.5 mol% TiO_2 addition. This result reveals the beneficial effect of the additive at the intergranular region by the substantial increase of the grain size, and consequent reduction of the blocking area. A further increase of the additive content to 5 mol%, in contrast, induces a small decrease of the grain boundary conductivity. In this case, the exsolution of the dopant from the solid solution may be responsible for the decrease of the grain boundary conductivity. This effect seems to be more severe at the intergranular region than in the bulk of sintered specimens.

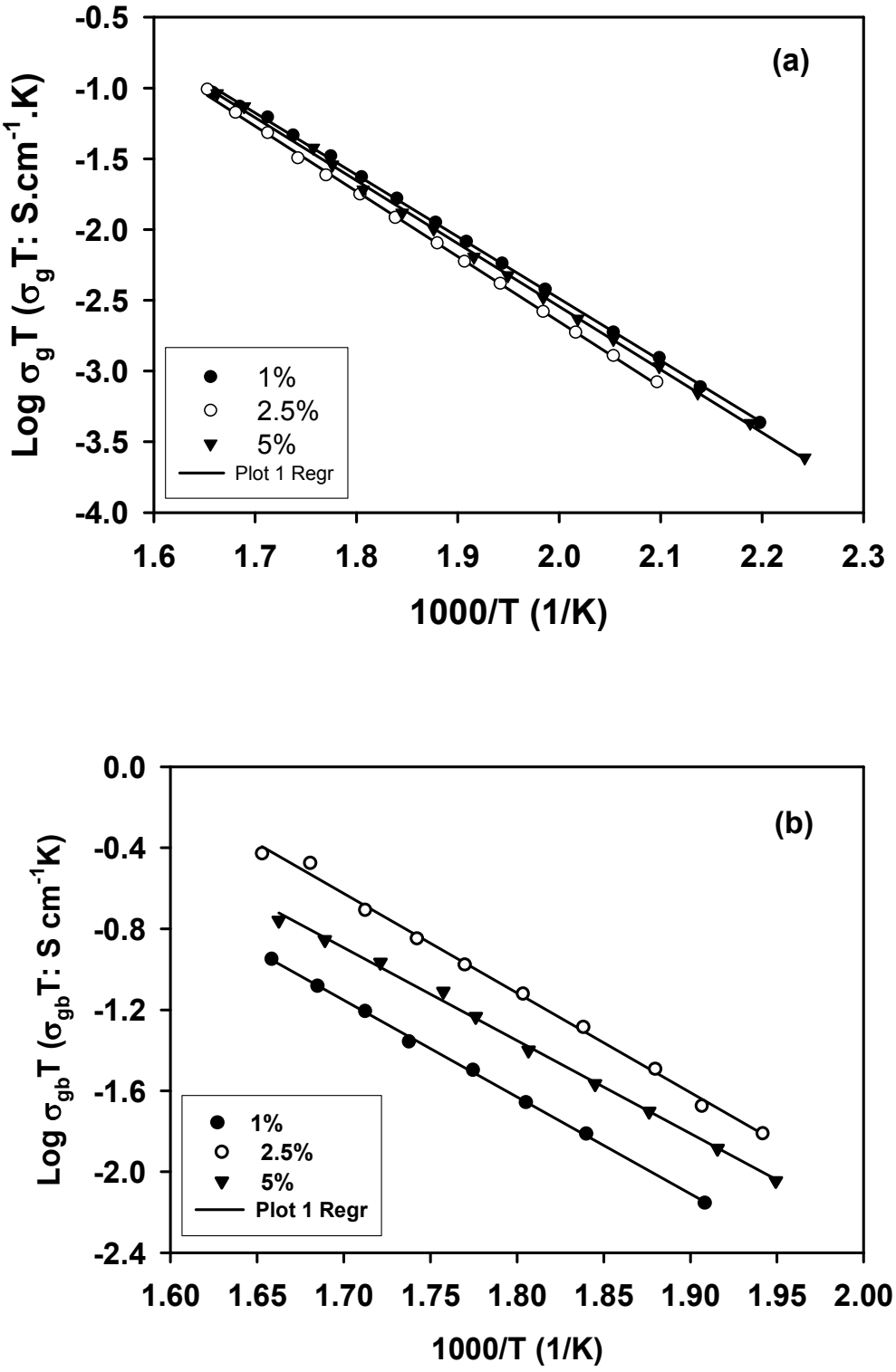

Figure 5. Arrhenius plots of the (a) grain and (b) grain boundary conductivity of TiO_2 containing gadolinia-doped ceria specimens.

The activation energy values determined for the grain and grain boundary conductivities are listed in Table 2. The values obtained for the grains are similar within the experimental

errors. For the grain boundaries, the activation energy values increase up to 2.5 mol% TiO_2. This effect is related to the addition of titania above the solubility limit. The activation energy of grain boundaries decreases with additional increase in the TiO_2 content (5 mol%) due to the formation of a more conductive phase ($Gd_2Ti_2O_7$) at the grain boundaries.

SUMMARY

Small additions of titanium oxide improved the densification and turned negligible the porosity of sintered gadolinia-doped ceria specimens. Full density was attained with the additive concentration of 5 mol%. Grain growth of the ceria solid electrolyte was promoted for additive contents up to 2.5 mol% with a consequent decrease in the boundary area. For higher concentrations of TiO_2 the grain growth was inhibited, due the formation of a secondary phase at the grain boundaries. This secondary phase was identified by Raman spectroscopy as $Gd_2Ti_2O_7$. The formation of Gd-containing secondary phase affects the grain and the grain boundary conductivity. The grain conductivity experiences a slight decrease with titania addition, because of the low solubility of the additive in the ceria matrix. The grain boundary conductivity increases with TiO_2 contents up to 2.5 mol% due to the decrease in the grain boundary area. For higher additive contents, the grain boundary conductivity decreases probably because of the secondary phase formed along the interfaces.

ACKNOWLEDGEMENTS

Financial support from FAPESP and CAPES are gratefully acknowledged.

REFERENCES

[1] A. Trovarelly, Catalytic Properties of Ceria and CeO_2-Containing Materials, *Catal. Rev. Sci. Eng*. **38**, 439-520 (1996).

[2] X. J. Yu, P. B. Xie and Q. D. Su, Size-Dependent Optical Properties of Nanocrystalline CeO_2: Er Obtained by Combustion Synthesis, *Phys. Chem. Chem. Phys*. **3**, 5266-5269 (2001).

[3] J. L. Macmanus-Driscoll, S. R. Foltyn, Q.-X. Jia, H. Wang, A. Senquis, I. Civale, B. Mairov, M. E. Hawley, M. P. Maley and D. E. Peterson, Strongly Enhanced Current Densities in Superconducting Coated Conductors of $YBa_2Cu_3O_{7-x}$+$BaZrO_3$, *Nature Mater*. **3**, 439-443 (2004).

[4] B. H. H. Steel and A. Heinzel, Materials for Fuel-Cell Technologies, *Nature* **414**, 345-352 (2001).

[5] N. Guillou, I. C. Nistor, H. Fues and H. Hahn, Microstructural Studies of Nanocrystalline CeO_2 Produced by Gas Condensation, *NanoStruct. Mater*. **8**, 545-557 (1997).

[6] S. Tsunekawa, T. Fukuda and A. Kasuya, Blue Shift in Ultraviolet Absorption Spectra of Monodisperse CeO_{2-x} Nanoparticles, *J. Appl. Phys*. **87**, 1318-1321 (2000).

[7] M. Yamashita, K. Kaneyama, S. Yabe, S. Yoshida, Y. Fujishiro, Y. Kawai and T. Sato, Synthesis and Microstructure of Calcia Doped Ceria as UV Filters, *J. Mater. Sci*. **37**, 683-687 (2002).

[8] H. Yahiro, K. Eguchi and H. Arai, Electrical Properties and Reducibilities of Ceria Rare Earth Oxides Systems and their Application to Solid Oxide Fuel Cells, *Solid State Ionics* **36**, 71-75 (1989).

[9] J. R. Jurado, Present Several Items on Ceria-Based Ceramic Electrolytes: Synthesis, Additive Effects, Reactivity and Electrochemical Behaviour, *J. Mater. Sci*. **36**, 1133-1139 (2001).

[10] R. A. Cutler, D. L. Meixner, B. T. Henderson, K. N. Huntchings, D. M. Taylor and M. A. Wilson, Solid Electrolytes and Electrical Interconnects for Oxygen Delivery Devices, *Solid State Ionics* **176**, 2589-2598 (2005).

[11] E. Yu. Pikalova, V. I. Maragou, A. K. Demin, A. A. Murashkina and P. E. Tsiakaras, Synthesis and Electrophysical Properties of (1-x)$Ce_{0.8}Gd_{0.2}O_{2-\delta}$+x$TiO_2$ (x=0-0.06) Solid-State Solutions, *Solid State Ionics* **179**, 1557-1561 (2008).

[12] J. R. McBride, K. C. Hass, B. D. Poindexter and W. H. Weber, Raman and X-ray Studies of $Ce_{1-x}RE_xO_{2-y}$, Where RE=La, Pr, Nd, Eu, Gd, and Tb, *J. Appl. Phys*. **76**, 2435- 2441 (1994).

[13] A. F. Fuentes, K. Boulahia, M. Hanuza and U. Amador, Synthesis of Disordered Pyrochlores, $A_2Ti_2O_7$ (A = Y, Gd and Dy), by Mechanical Milling of Constituent Oxides, *Solid State Sci*. **7**, 343-353 (2005).

[14] H. Yahiro, K. Eguchi and H. Arai, Ionic-Conduction and Microstructure of the Ceria-Strontia System, *Solid State Ionics* **21**, 37-47 (1986).

[15] A. L. Horovistiz and E. N. S. Muccillo, Microstructural and Electrical Characterizations of Chemically Prepared $Ce_{0.8}Gd_{0.2-x}(Ag, Sr)_xO_{1.9}$ ($0 \leq x \leq 0.03$), *Solid State Ionics* **225**, 428-431 (2012).

[16] M. Mori, E. Suda, B. Pacaud, K. Murai and T. Moriga, Effect of Components in Electrodes on Sintering Characteristics of $Ce_{0.9}Gd_{0.1}O_{1.95}$ Electrolyte in Intermediate-Temperature Solid Oxide Fuel Cells During Fabrication, *J. Power Sources* **157**, 688-694 (2006).